Environmental Advances 16 (2024) 100536

Contents lists available at ScienceDirect

Environmental Advances

journal homepage: www.sciencedirect.com/journal/environmental-advances

First evidence of anthropogenic TiO_2 nanoparticles occurrence in Chilean rivers

Gester G. Gutiérrez [a,b,*], Alessandra Perfetti-Bolaño [a], Manuel Meléndrez [c,d], Karla Pozo [e,f], Ilaria Corsi [g], Ricardo O. Barra [a], Roberto Urrutia [a]

[a] Facultad de Ciencias Ambientales y Centro EULA Universidad de Concepción, Chile
[b] Departamento de Química Ambiental, Facultad de Ciencias, Universidad Católica de la Santísima Concepción, Concepción, Chile
[c] Interdisciplinary Group of Applied Nanotechnology (GINA), Hybrid Materials Laboratory (HML), Department of Materials Engineering (DIMAT), Faculty of Engineering, University of Concepcion, 270 Edmundo Larenas, Box 160-C, Concepcion 4070409, Chile
[d] Facultad de Ciencias para el Cuidado de la Salud, Universidad San Sebastián, Campus Las Tres Pascualas, Lientur 1457, Concepción 4060000, Chile
[e] Masaryk University, Faculty of Science, RECETOX, Brno, Czech Republic
[f] Universidad San Sebastián, Facultad de Ingeniería, Arquitectura y Diseño, Lientur 1457, Concepción, Chile
[g] Department of Physical, Earth and Environmental Sciences, University of Siena, Italy

ARTICLE INFO

Keywords:
TiO_2 nanoparticle
Surface water
Nanowaste
Pollution
Field study

ABSTRACT

This study marks the first recorded case of TiO_2 nanoparticle pollution in Chilean rivers, indicating significant progress in understanding the distribution of nanowaste and its effects on a global scale. By investigating four different locations, including the outlet of a wastewater treatment plant during summer, winter and spring, the research revealed varied concentrations of TiO_2 nanoparticles, with a notable range between 17.6 μg L^{-1} during the summer and 22.9 μg L^{-1} in spring in downstream river sections. The study used transmission electron microscopy to characterize nanoparticles, observing sizes between 10 and 206 nm, and an EDS detector confirmed titanium proportions of 4.84 % to 20.35 % by dry weight. These TiO_2 nanoparticles, predominantly in Rutile and Anatase forms, denote a significant environmental presence, especially considering the low population densities of the sampling areas. The findings highlight the urgent need for international awareness and routine monitoring of nanowaste, advocating for preventive actions in the production of nanomaterials and adaptive management strategies in tune with the dynamic nature of water systems and environmental changes, both for places densely and sparsely populated.

1. Introduction

Over time the nanotechnology industry has become among the most versatile, improving various chemical substances with unique properties according to their use, function, and fate (Yadav & Ahmaruzzaman, 2022). The characteristics according to which these substances are classified as nanoparticles are size below 100 nm and defined structures with specific functions that form molecular agglomerates or aggregates with weak or strong bonds that allow them to react with other components of the medium (Ale et al., 2019; Cascio et al., 2015; Zhang et al., 2022). However, the efficacy and long-term stability of these nanoparticles remain poorly understood, particularly for those engineered with a specific application in mind without adequately considering their eventual environmental disposal. This gap in understanding represents a potential environmental hazard, as the oversight of post-use disposal practices can lead to ecological disturbances. Such disruptions may contribute to imbalances in natural processes, affecting ecosystem homeostasis (Banerjee & Roychoudhury, 2019; Deng et al., 2017; Fan et al., 2019; Kim et al., 2011; Oukarroum et al., 2013; Stegemeier et al., 2017).

In recent years, TiO_2 nanoparticles have been incorporated into various everyday and domestic products. They can be found in cosmetic additives (Morais et al., 2022), medications (Farshbaf et al., 2022), and foods (dos Santos et al., 2020). TiO_2 has chemical stability properties as an amphoteric oxide, and is an n-type semiconductor, which makes it sensitive to light, absorbing mainly UV radiation, making it the most used photocatalyst to degrade organic molecules. It is also used as a white pigment, anticorrosive coating, gas sensor, UV-ray absorber in

* Corresponding author.
E-mail address: gesgutierrez@udec.cl (G.G. Gutiérrez).

https://doi.org/10.1016/j.envadv.2024.100536
Received 11 February 2024; Received in revised form 1 April 2024; Accepted 15 April 2024
Available online 16 April 2024

cosmetic products, and generally in the ceramic industry (Khan et al., 2020, 2023; Rai et al., 2019).

Synthetic nanoparticles of TiO_2 lack trace elements within their structure and typically exhibit a size below 100 nm, white pigmentation, and an isoelectric point less than 3. Their composition primarily consists of anatase and/or pure rutile, sometimes coated with small amounts of aluminum and/or silica to enhance technological properties. The affinity of these nanoparticles with organic matter is contingent upon the type of surfactant they are associated with. Consequently, one can anticipate the presence of nanoparticulate structures associated with various forms of organic matter, including lipids or in their free form (Campos et al., 2022; Liao & Liao, 2007). TiO_2 nanoparticle production accounts for around 37 % of total nanoparticle production, and it is one of the most used nanomaterials worldwide (Yadav & Ahmaruzzaman, 2022); this statistic implies a high probability that TiO_2 will be found as waste in natural water bodies due to increases in the use of these products (Keller et al., 2010).

There are studies that show the existence of these nanoparticles downstream of urban settlements (Bäuerlein et al., 2017). Complementarily, anthropogenic input of TiO_2 nanoparticles through wastewater treatment plants inside and outside the facilities has been reported in different parts of the world (Westerhoff et al., 2011), as well as their input through water runoff of rain to different river systems (Boenisch, 2020; Nabi et al., 2021). The quantification and identification of nanoparticles allow evaluating the long-term effects on ecosystems exposed to TiO_2 nanoparticles; This information can help define possible scenarios after the release of nanoparticles to the environment, considering bioavailability and transport in aqueous solutions. In Chile it has been shown that existing wastewater treatment systems do not have adequate technology to eliminate emerging contaminants (Rozas et al., 2016). Therefore, it does not guarantee that nanowaste is removed within the system. Furthermore, there is an information gap due to the lack of studies on nanopollutants, so there is not enough evidence to expand current regulations and prevent the degradation of the water available in Chile for consumption, this being an important issue to address, especially in through new scenarios due to the effect of climate change. The Biobío River is one of the main rivers in Chile, it has a network of rivers that contribute to the drainage basin and has a high socioeconomic value for the region and the country, providing various ecosystem services, including water extraction for irrigation in the agricultural and forestry industry, drinking water supply and hydroelectricity. energy production, among others (Díaz et al., 2018). Currently, the Biobío basin supplies drinking water to 1.2 million people, who in turn discharge domestic water through the main wastewater treatment plants, closing the cycle of use and reuse of this resource. This is why it is important to quantify the life cycle of TiO_2 nanoparticles, considering that there is currently no monitoring of the consumption of the products that contain them, so it is necessary to know the quantities and ways in which they enter the systems. aquatic after its application.

The objective of this study is to explore the presence of TiO_2 nanoparticles in one of the main rivers of Chile, determining the concentrations, morphologies and sizes of these nanoparticles.

Furthermore, the study seeks to evaluate the environmental influence on the origin of TiO_2, differentiating anthropogenic and natural sources.

2. Material and methods

2.1. Study area and samples collection

Situated in south-central Chile, the Biobío River spans between latitudes 36°42′ S and 38°49′ S, and longitudes 71° W to 73°20′ W, covering a catchment area of 24,264 km^2. At 380 km in length, it stands as one of Chile's largest basins. Its hydrological profile is complex, featuring nival origins in the Alto BíoBío region and pluvial contributions in its middle course, which often result in seasonal flooding, predominantly in the winter and spring months (Caro, 2004). Human activities variably impact the river along its course, exploiting its resources for a range of purposes. This is set against a backdrop of significant biological processes and hydrodynamic shifts that are seasonally driven.

This study examines the influence of human activities on nanoparticle dissemination in the Biobío River, integrating both anthropogenic and natural seasonal fluctuations. Sampling was strategically conducted in line with the distinct climatic seasons of the southern hemisphere—specifically during the summer, winter, and spring of 2022. The research was carried out at four key locations along the river: Alto BíoBío, Santa Bárbara, Hualqui, and Hualpén, chosen to elucidate the gradient of contamination. Annex A in the supplementary materials provides a comprehensive overview of the sampling sites, methodologies, and results, complete with detailed Tables and figures

At each sampling site, 3 surface water samples were collected no more than 30 cm from the surface in 1 L amber glass bottles in triplicate and in 10 L HDPE-quality plastic jugs. Before their use, the bottles and jugs were washed with phosphate-free neutral detergent and then with 10 % hydrochloric acid (Sigma Aldrich, EMSURE® ACS, ISO, Reag. Ph Eur) for at least 24 h. They were subsequently rinsed three times with running water and then submerged in ultrapure water (Easy pure, Centro-EULA, Chile) for 24 h. To dry the glass bottles, they were kept in a stove at 60 °C for another 24 h. The jugs were dried in open air face down, avoiding contact with any type of trace contaminants, for 24 h. During the sampling, before each sample was taken the bottles and jugs were primed three times with surface water from each sampling point before the definitive water samples were taken. The bottles with samples were handled with nitrile gloves to avoid any contamination from outside the sampling location. The samples were stored in the dark at 4 °C until further analysis.

2.2. ICP and ICP-MS analysis

The methodology for sample preparation and elemental analysis via ICP-MS and ICP was carried out with precision. Initially, the samples were subjected to digestion: each was homogenized and placed in Teflon containers, each with a capacity of 50 mL. To this, 3 mL of Suprapur® concentrated nitric acid was added. The mixture was then heated until the volume was reduced to 10 mL. Subsequently, the concentrates were transferred to 50 mL plastic volumetric flasks, supplemented with an additional 5 mL of nitric acid, and then diluted to the marked volume with ultrapure water.

Elemental concentrations of titanium (Ti), with a limit of detection (LOD) of 0.02 μg L^{-1}, niobium (Nb, LD 0.001 μg L^{-1}) and vanadium (V, LD 0.085 μg L^{-1}) were quantified. These analyzes aimed to distinguish natural titanium dioxide (TiO_2) nanoparticles from those of anthropogenic origin, following the approach suggested by Nabi (2021). The determination was carried out using an ICP-MS (Thermo Scientific iCAP RQ). Additionally, iron (Fe, LD 1 μg L^{-1}), manganese (Mn, LD 1 μg L^{-1}) and aluminum (Al, LD 5 μg L^{-1}) were incorporated into the study and evaluated by ICP using an optical emission spectrophotometer (Perkin Elmer Optima 8000).

Calibration of the analytical instruments was performed using Certipur $TiCl_4$ in HCl (1000 ± 2.00 g L^{-1} Ti), a vanadium (V) ICP standard (1000 mg L^{-1}) and a niobium (Nb) standard (1000 ± 5 μg mL^{-1}). In a mixture of nitric and hydrofluoric acid). Multielement standards for Fe, Mn, and Al were used for ICP analysis (Baird & Bridgewater, 2017).

2.3. Nanoparticle detection using TEM and VP-SEM with EDS detector

The methodology for nanoparticle observation and analysis used a Talos F200 G2 transmission electron microscope (Thermo Scientific) equipped with a high-resolution CETA 16M CMOS camera. This configuration, including an in 3D.

Sample preparation involved triplicate transfers to 50 mL Falcon tubes, followed by a 10 min sonication period. This was followed by a

tiered centrifugation protocol: 500 rpm for 4 min, 3500 rpm for 5 min and finally 5000 rpm for 30 min, with meticulous pipetting of the sample after each step, as recommended by Phillipe et al. (2022). Samples were then mounted on Formvar/carbon coated TEM 200 mesh copper grids and dried at 60 °C, 10 μL drops were concentrated onto the grid as many times as necessary to ensure a smooth and homogeneous grid surface. low magnification.

The comparative analysis used a titanium (IV) oxide standard (mixture of rutile and anatase, particle size < 100 nm) prepared at 10 μg L^{-1} for TEM observation, following the same procedures applied to the water samples.

Additional observations were made using a Zeiss EVO MA10 variable pressure scanning electron microscope (VP-SEM) with an Oxford x-act EDS detector, where AZtec 6.0 SP1 software facilitated data analysis. Samples were coated with carbon to a thickness of 10 nm and spot spectra were acquired using automated settings over a period of 6 min.

For nanoparticle dimension analysis, ImageJ version 1.54c, a Java-based open source imaging software, was used.

2.4. Statistical analyses

The Shapiro–Wilk test was applied to assess the normality of the data distribution of each recorded variable. In addition, Kruskal–Wallis was used to determine the existence of statistically significant differences in the recorded variables according to the "Location" and "Season" factors. Finally, an analysis of variance (ANOVA) was carried out to determine the existence of statistically significant differences in the recorded variables according to the "Location" and "Season" factors. The program used was Statistical analysis was conducted using R Studio version 4.3.1.

3. Results and discussion

In the four sampling points studied, a clear similarity was evident according to their physicochemical characteristics and seasonal variations (summer, winter and spring) in the Alto Biobio and Santa Bárbara sites located in the upper middle zone of the river, according to the recorded field data. The same similarity is observed in the Hualqui and Hualpén sampling points located in the lower part of the river. However, these last two points differ from the two points mentioned above. These differences stand out even more when the factor of the gradient of urban activity is considered, since as one advances along the course of the river, urban settlements increase and with it the discharges from the treatment plant into the river (Vera et al., 2013). Therefore, the Hualqui and Hualpén sampling sites are the ones with the greatest urban influence because the main wastewater treatment plants are located, and according to the information provided by the Superintendence of the Environment (2019), they treat the domestic waters of more than 559, 908 inhabitants (To view the map and location of the sampling points, see Fig. 1 of Annex A in supplementary material).

In Fig. 1 (dendrogram), the previously mentioned observations are visually depicted. A sizable cluster encompasses all the assessed localities along the Biobío River, emphasizing the notable similarity between the localities of Alto Biobío and Santa Bárbara across multiple stations. Within the second group, comprising the towns of Hualqui and Hualpén, a substantial divergence is evident during winter compared to the rest of the localities.

The dendrogram clearly illustrates the subdivision of the four sampling points based on their chemical and physical characteristics into two distinct groups. The upper-middle course is characterized by the grouping of Alto Biobío and Santa Bárbara, while the lower course of the Biobío River accommodates the points of Hualqui and Hualpén.

3.1. ICP-MS analyses

The ICP-MS analyzes of the water samples showed the presence of total Ti in all sites in concentrations of the order of μg L^{-1}, with higher concentrations found in Alto Biobío in summer 24.6 μg L^{-1}, Hualqui in winter 39.5 μg L^{-1} and Hualpén in spring 22.9 μg L^{-1} (Fig. 2). The analysis carried out for total Ti, Al, Fe, V, Nb and Mn, in surface waters, shows the existing profile in the sampling areas, with the predominant presence of Fe and Al and, to a lesser extent, Mn, while for Nb and V values were below the detection limit. It is important to describe the concentration of the elements mentioned above to contrast with Ti and thus be able to establish the possible origins of TiO_2 present in the surface water (Vidmar et al., 2022).

Fig. 2 illustrates the fluctuation in total Ti concentrations (left Y-axis) along the river in correlation with measured flow (right Y-axis), during summer, winter, and spring. The summer data reveal a gradual increase in Ti concentrations from Santa Bárbara to Hualpén, this coincides with the decrease in flow in this period of the year, evidencing the concentrations of solutes in the river. However, surprisingly, in Alto Biobío, characterized by minimal human interference, in the same season the

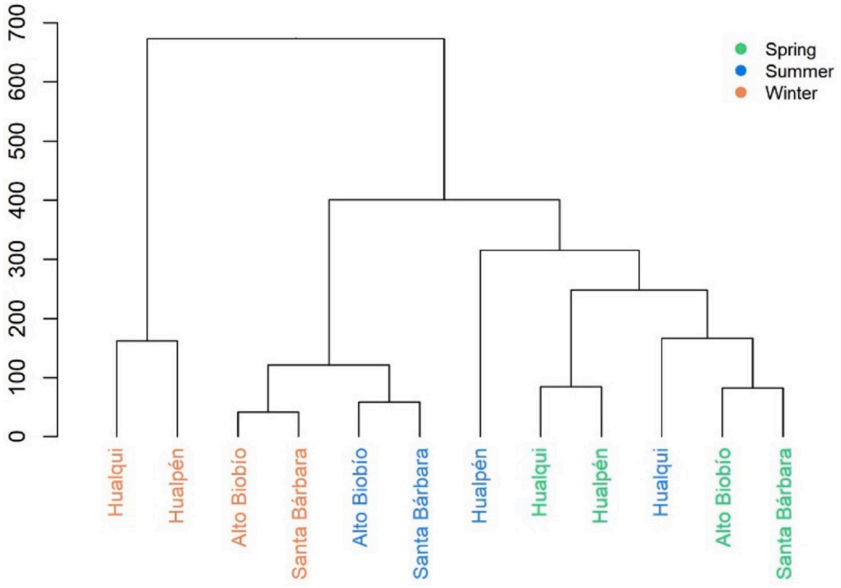

Fig. 1. Similarity analysis (dendrogram) based on untransformed data matrix of variables recorded in surface water at different locations along the course of the Biobío River in different seasons.

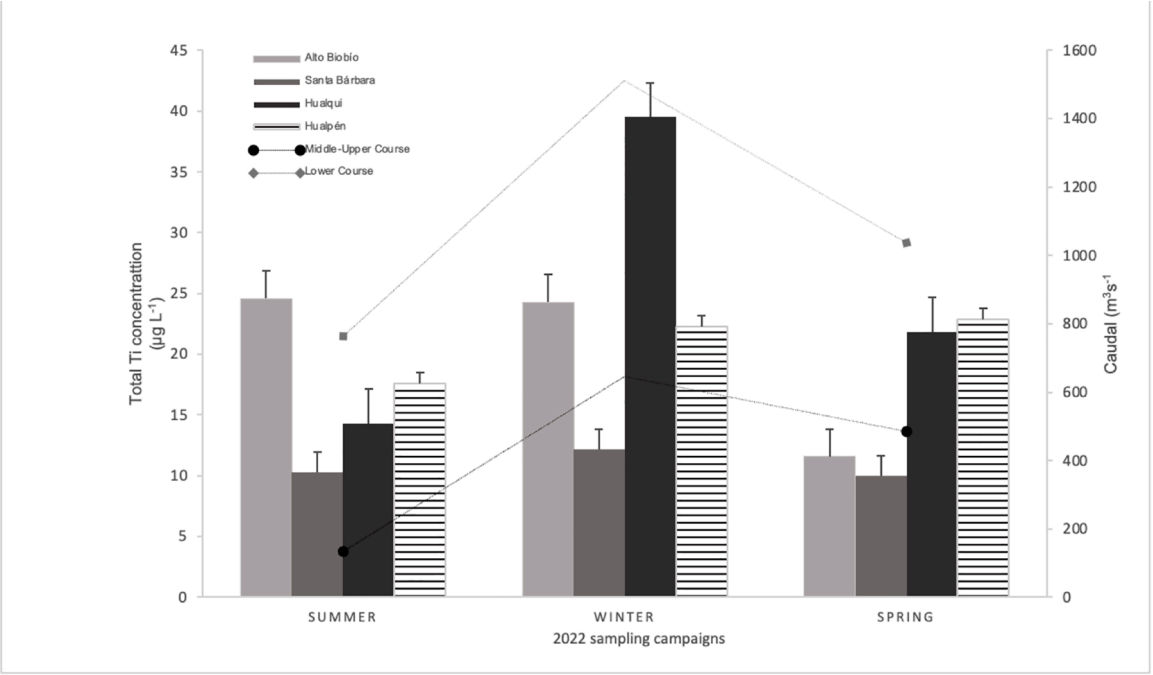

Fig. 2. Total Ti results obtained via ICP-MS by campaign in the Biobío River and flows at the different sampling points; from left to right: Alto Biobío, Santa Bárbara, Hualqui, Hualpén. The standard error bar represents the analysis of three samples taken at the same sampling point in each season.

highest concentration was recorded with 24.6 µg L^{-1}.

This unexpected result may be attributed to the influence of Ti concentration resulting from ice melting on the mountain. With a river flow of 135 m^3 s^{-1}, the lowest among all points measured, the Ti peak could be linked to atmospheric transport of nanoparticles from urban areas. These particles may condense and encapsulate in the coldest mountain points during winter, subsequently releasing between spring and summer.

This hypothesis finds support in the research of Azimzada et al. (2020), which highlights climatological influences, particularly in cold climates, on the transport of TiO_2 nanoparticles (Azimzada et al., 2020). On the other hand, it should be noted that in Andean areas at the sampled points, the type of soil through which the river passes contains Ti minerals in nature, highlighting magnetite-ulvöspinel (Fe_2TiO_4) and ilmenite-Hematite ($FeTiO_3$).

According to a report from the National Geological Service of Chile in 2003, the soil formations present in the basin influence the composition of the water that flows over the territory. The upper part, where the river originates, is composed of sedimentary volcanic rocks, sandstones, paraconglomerates, andesitic and dacitic lavas and intercalations of ignimbrites, limonites and limestones. The soils are mainly composed of OM2c, KT2 and PPI3 and according to these geological codes (see Fig. B in supplementary materials) these have high Fe contents and formation of Fe oxides, explaining the high concentrations of Fe found in surface waters, these soils being the main soils that They naturally present Fe-Ti interactions (Henriquez, 1978). Furthermore, according to reports from the General Directorate of Water of Chile (DGA, 2022), in this area of the upper middle course the flow is much lower than at the mouth of the river (Fig. 1); Therefore, there is an effect of the concentration of Ti in the area. According to this effect and considering the effects of evaporation in summer, it would be interesting in a future study to sample Andean lakes to analyze the possibility of nanoparticles arriving through atmospheric transport. In the midstream Santa Bárbara region, analysis of variance of Ti, Al, and Fe concentrations (Fig. 4) demonstrated minimal seasonal fluctuation, with Ti levels remarkably consistent, ranging only between 10 and 12 µg L^{-1} throughout the year. This stability likely reflects river flow dynamics and local soil composition, suggesting that the Santa Bárbara site can serve as a reference point for establishing natural background levels against which contamination can be measured. Therefore, future studies should consider incorporating an upstream sampling location to differentiate between baseline Ti contributions from the Alto Biobío region and potential nanoparticle contaminants arising from urban activities in Santa Bárbara. The third sampling site is located in Hualqui, located in the lower part of the river basin. At this sampling point, the highest Ti concentration is found in winter (39.5 µg L^{-1}) compared to the other sampling points sampling. This is not unexpected, since upstream of Hualqui is the confluence of another important river in the hydrographic basin that contributes to the main course of the Biobío River. This has a spring with soil formation characteristics similar to the Biobío River, it rises in a lake located in the middle of volcanic sequences where other studies reported the existence of TiO_2 concentrations (Vera et al., 2013). Another important factor to consider is that this tributary river also receives interactions from large cities located in the middle course of the region and that could enhance the contributions of Ti (Albornoz Tapia, 2019). Therefore, the Ti peak observed at the Hualqui sampling point is not surprising, especially in winter due to precipitation that contributed to an increase in the flow of the Laja River of around 700 mm $year^{-1}$ in 2022 (DGA, 2022), which could drag these particles towards the Hualqui area.

At the last sampling point, few of the Ti contributions observed could be of natural origin, since the soil in the area is of type CPg and Q1, formed by conglomerates, breccias, sandstones, shales and limestones that interact with contributions of Ca and Si, not related to basaltic soils linked to oxide minerals that affect natural Ti contributions; Therefore, the Ti concentrations observed in Hualpén in summer (17.6 µg L^{-1}), winter (22.3 µg L^{-1}) and spring (22.3 µg L^{-1}) are mostly of anthropogenic origin.

The mixed behavior of the sampled river, with increases in flow in spring and winter, makes it difficult to establish a relationship between anthropogenic and natural contributions of Ti. The use of Fe and Al for the normalization of Ti allows us to date the natural and anthropogenic contributions of Ti (Fig. 3) in summer, winter and spring. When contrasting this information with spatial analysis (Fig. 4) of the

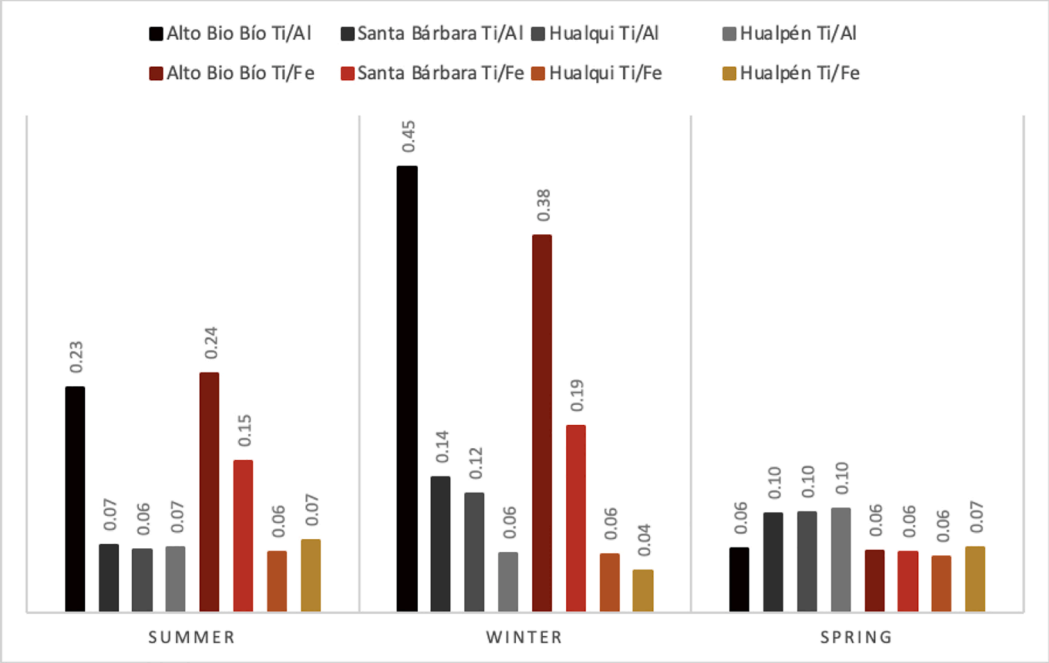

Fig. 3. Ti/Al element ratio in grayscale and Ti/Fe in red scale; variations by season and sampling point are shown.

concentrations of Ti, Al, Fe and Mn, a marked trend of lower variability is observed in the upper course of the Biobío River compared to the lower course, where the Hualqui points are located and Hualpén. Additionally, an increase in the concentration of Al and Fe was observed along the course of the river to the lower part. On the other hand, for Ti, in Hualpén an increase in concentration is observed as time passes during 2022. This information reveals and confirms a greater influence of anthropogenic contributions that are enhanced by temperature gradients in different areas. sampled. The temperature contrast in the lower part of the river is between 0.3 and 5 °C greater than in the upper course, which causes greater evaporation of water. Furthermore, increasing drought conditions have been recorded in the area in recent years, decreasing the amount of water available and at the same time concentrating solutes in the river (Yevenes et al., 2018). Such consequences of climate change are among the important reasons. Regulate and control emissions of micropollutants that enter aquatic systems with characteristics similar to the Biobío River.

In a future study it would be important to complement this research with isotopic analyzes of the elements Ti, Al and Fe to more precisely trace their origins. For their part, these results coincide with studies on contributions from soils and rivers carried out in other parts of the world, in which it has been estimated that the proportion of TiO_2 in minerals is approximately 0.25-0.95 % of the total, a very low figure. percentage (Greber et al., 2021). Despite the difficulty in interpreting the origin of the TiO_2 nanoparticles, these data allow inferences to be made about the sampling points that are important to consider to construct an adequate mineralogical baseline and to be able to trace the origins of the dual-origin nanoparticles that enter the rivers. with characteristics similar to those of the Biobío River.

Another tracer of the anthropogenic origin of TiO_2 nanoparticles is Mn. This is related to TiO_2 nanoparticles, since it is used in the doping of synthetic anatase and rutile structures (Sukhdev et al., 2020), for energy harvesting and storage products (Latif et al., 2022), dyes and disposal in the paper industry (Mohamed et al., 2007). The results obtained by the ICP-MS show that for the points of Alto Biobío and Santa Bárbara where Ti is strongly related to natural sources, since the Mn quantified for those points is below the detection limit in the summer months and winter, which would corroborate that the nanoparticles present are not related to an anthropogenic origin, however in the same sampling seasons, in the sites of the lower course of the river, concentrations between 12.3-19.6 μg L^{-1} could be detected. 1 of Mn marking the existence of statistically significant differences between sampling stations determined by the Kruskal-Wallis test (see Table in annex c), in addition the concentrations of Mn present statistically significant positive relationships with conductivity.

According to field observations, between the Santa Bárbara and Hualqui points, the activity in areas near the river is industrial, with pulp plants and the active construction (2023) of a series of wind farms in areas that directly impact the Biobío River and its tributary rivers. These industrial activities could explain the increase of Ti in water samples.

In the principal components graph (Fig. 5), Axis PC1 reflects 80.22 % of the total variance, explained by the variability of the concentrations of Fe and Al, which according to the ordination analysis appear to be different between localities in the upper middle zone and the lower zone of the Biobío River. Furthermore, the variance captured by the PC2 axis (16.52 %) reflects the variability in conductivity values in Hualqui and Hualpén between different stations. This could be a consequence of the concentrations of solutes in the lower area of the river, where there is also estuarine influence, since the Hualpén sampling point is located almost at the mouth of the Biobío River.

In this sense, soils can represent a source of nanoparticles for the surface water of the Biobío River. For example, in agriculture, Fe nanoparticles are used to increase nutrient absorption and germination (Santás-Miguel et al., 2023). Consequently, the application of nano-agrochemicals could increase their content in the soil and crops (Rajput et al., 2021). According to the CONAF Territorial Information System, Hualqui covers an area of 2,694 hectares of agricultural land (Corporación Nacional Forestal, 2020). This site could represent a seasonal source of nanoparticles transported by runoff with winter precipitation, which could end up into river watersin Hualpén.

3.2. *TEM analysis*

To analyze the TiO_2 nanoparticles through TEM in the surface water samples, the shapes and sizes of the standard of Titannium (IV) oxide nanoparticles, mixture of rutile and anatase at 10 μg L^{-1} in MilliQ water were compared (Fig. 6 A and B). The first observation in the prepared standards is the agglomerates of different defined shapes found in the

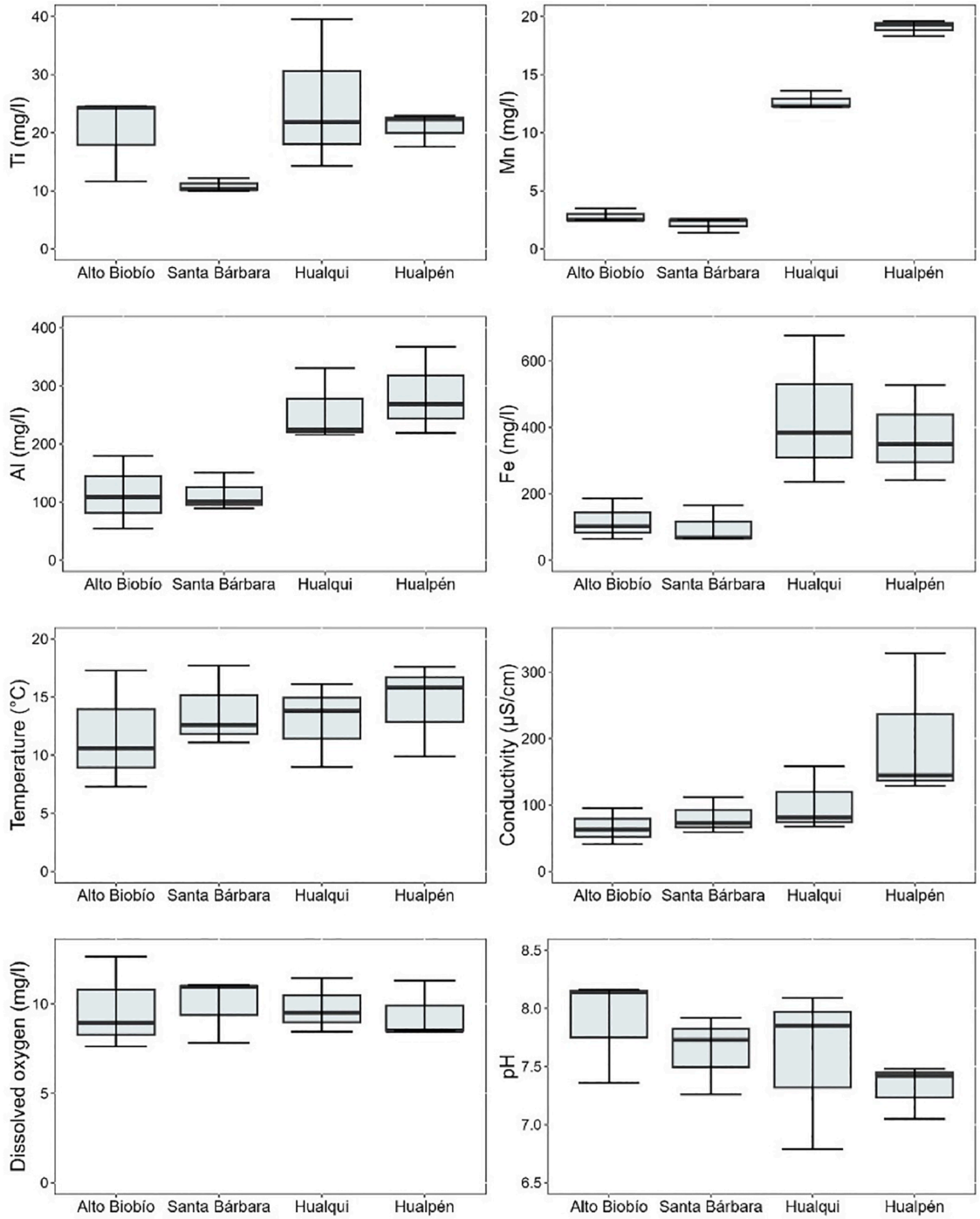

Fig. 4. Spatial variation of the most representative variables recorded in surface water along the course of the Biobío River. The locations are presented by decreasing elevation from left to right. Center lines in the boxes represent mean values.

standards, ranging from sizes < 100 nm as individual nanoparticles to > 100 nm in agglomerates. Despite these observations, it is possible to identify the forms of anatase (Fig. 6-A) and it is more difficult to identify Rutile (Fig. 6-B) according to the Bravais lattices (Iadonisi et al., 2014; Sengupta & Sarkar, 2015).

Regarding surface water samples, nanoparticle structures were found less frequently in the Alto Biobío; However, those that were observed were cubic (Fig. 6-C) and oval (Fig. 6-D) in shape, with sizes in the range between approx. 120–230 nm. These structures are associated with the organic matter of the samples, which is expected since TiO_2 nanoparticles of natural origin tend to be hydrophobic and have a greater affinity for this matter, unlike manufactured TiO_2 nanoparticles that have a wide coating variability. which can be hydrophilic or hydrophobic (Campos et al., 2022).

At the Santa Bárbara sampling point it was more common to find defined structures of TiO_2 nanoparticles in nanometric sizes < 100 nm. The observed nanoparticles were in individual states with tetragonal shapes characteristic of Anatase with one side with a size of 46 nm (Fig. 6-E) and tetragonal agglomerates characteristic of Rutile (Fig. 6-F). These shapes are consistent with TiO_2 nanoparticle structures synthesized using Pechini methods (Hajizadeh-Oghaz, 2019; Vargas Urbano et al., 2011). According to field observations, the sampling site was influenced by camping activities, so the presence of the observed nanoparticles is a consequence of this activity, identifying Santa Bárbara

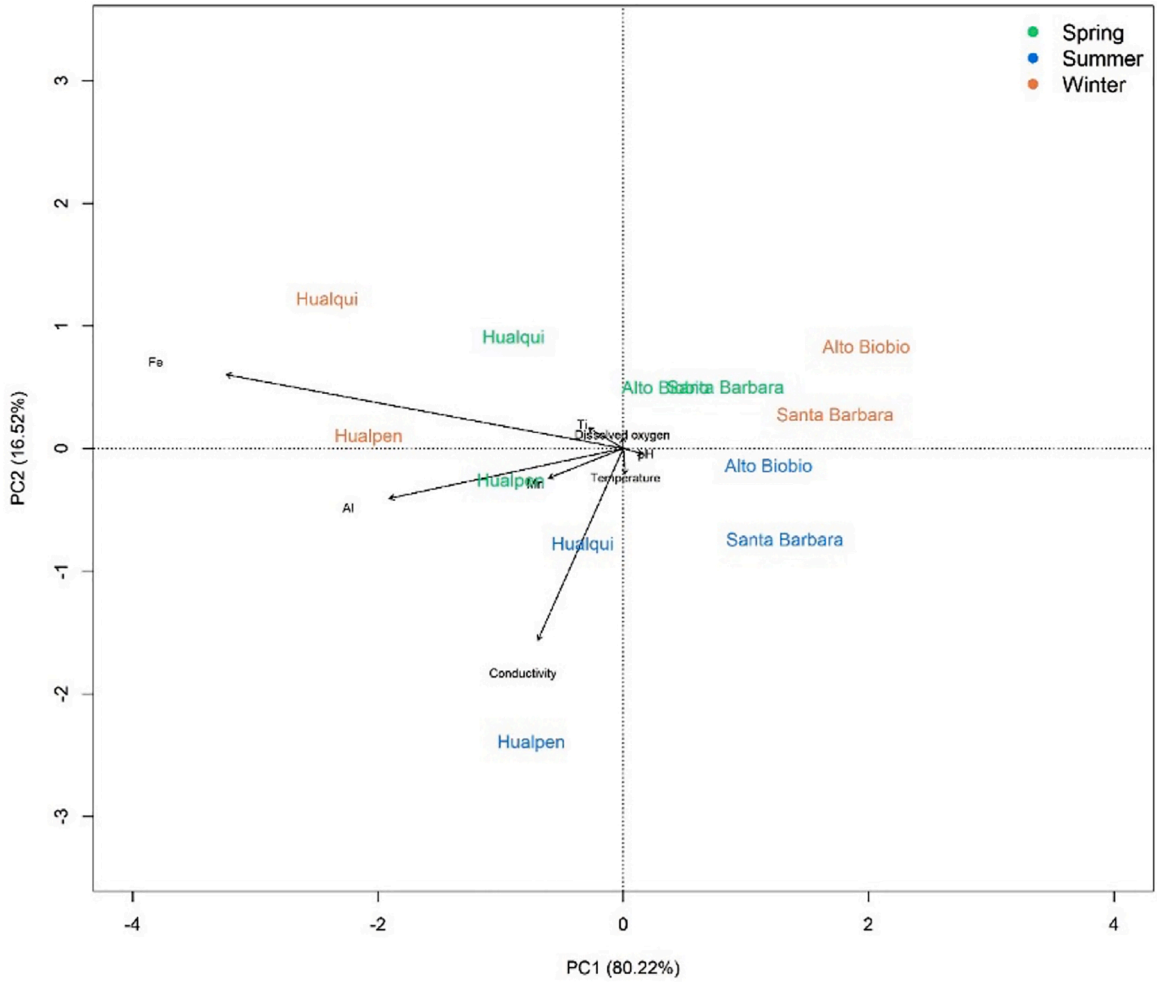

Fig. 5. Principal component analysis (PCA) based on variables recorded in surface water at different locations along the course of the Biobío River in different seasons, represented by different colors.

as the first point in this study where the entry of TiO_2 nanoparticles from recreational activities on the river.

At the Hualqui sampling point (Fig. 6-G,H,I and J) nanoparticle structures were observed more frequently than in Alto Biobío and Santa Bárbara, observing different types of structures that coincide with some observed at the previous points. Fig. 6-D and J show shapes and sizes that agree with those observed in the Alto Biobío, with a size of approximately 229 nm (Fig. 6-D) and 259 nm (Fig. 6-J), while Fig. 6 G and H, and show similarity to the homoagglomerate observed at the Santa Bárbara sampling point (Fig. 6-F), with a size of < 100 nm each. However, in Hualqui heteroagglomerated forms are observed, as seen in Fig. 6 G and I, where the nanoparticles are superimposed in different ways, which can be explained because at this point there is an increase in conductivity due to the concentration of solutes in the area, along with an increase in pH that promotes heteroagglomeration of nanoparticles (Labille et al., 2015). It is important to describe this, since these conditions promote the interaction of nanoparticles with other components in the environment, such as organic matter (Fig. 6-H), heavy metals, emerging contaminants and any other compounds present in surface water, increasing the probability of ecological risks. as the negative effects of settleable colloidal nanoparticles increase (Morelli et al., 2018), causing interaction with substrate-removing species that forage or bury themselves in the sediment (Bhagat et al., 2020).

This mixture of structures found in Hualqui is consistent with the increase in total Ti concentrations found at this sampling point, showing the coexistence of TiO_2 nanoparticles of natural and anthropogenic origin. Although TEM and ICP-MS analyzes are not sufficient to distinguish between the two origins (Philippe et al., 2018), it is possible to demonstrate their existence at sizes < 100 nm and larger.

Regarding the last stretch of the river, at the Hualpén sampling point, nanoparticle structures were observed more frequently, especially in summer and spring. The observed nanoparticle structures are well defined and have sizes between 50–200 nm. In this area there is a direct discharge from a wastewater treatment plant, which provides tangible evidence that the synthetic nanoparticles contained in everyday products are not retained during domestic water purification processes, and enter aquatic ecosystems without any filter type. Fig. 6-K, L, M and N show nanoparticles with very defined tetragonal and octahedral shapes, with a length range of approximately 85–120 nm. These structures can be clearly seen in the anatase and rutile phases. Rhombohedral shapes characteristic of the brookite TiO_2 phase are also seen (Fig. 6-K and N). The anatase octahedrite structures are slightly larger than those of rutile and share structural similarities, as stated by Akakuro (2020). If we compare the frequency of nanoparticle sightings at this sampling point with the total Ti concentration determined (Fig. 2), it can be concluded that the concentration of TiO_2 nanoparticles at this point is approximately 17.6-22.9 $\mu g\ L^{-1}$ between summer and spring. Furthermore, fewer agglomerates of nanoparticles and more defined structures are observed than the colloids observed in the Alto Biobío (Fig. 6-D).

To finish verifying the existence of the TiO_2 nanoparticles observed, SEM-DLS analysis was carried out on the surface water samples. These analyzes confirmed the Ti content in them, in quantities between 4.84 %

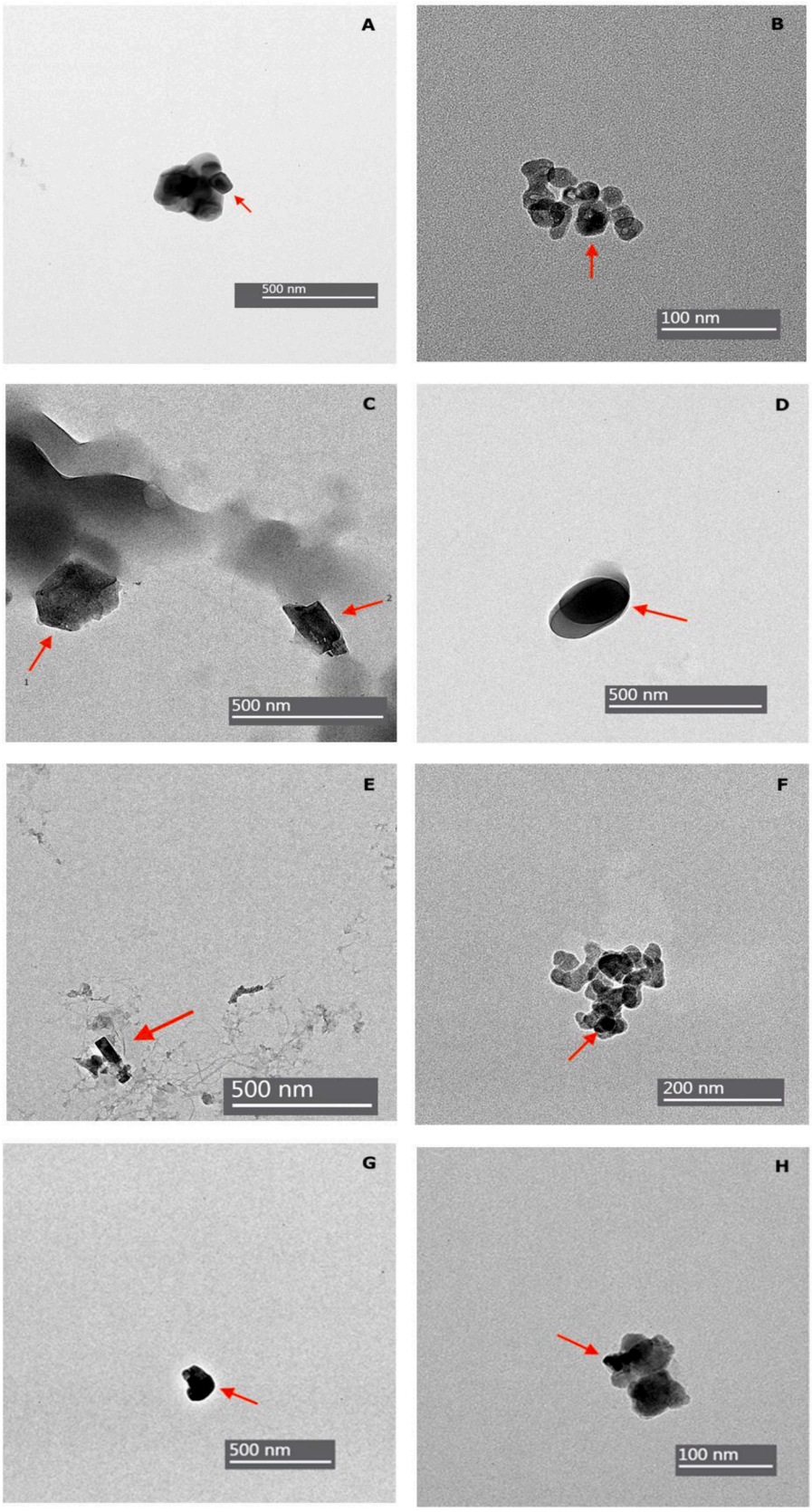

Fig. 6. Transmission electron microscope (TEM) analysis of standard of Titannium (IV) oxide nanoparticles, mixture of rutile and anatase (MKCR1332) and of surface water samples at each sampling point: A and B: anatase and rutile standards at concentrations of 10 μg L^{-1} and size < 100 nm; C and D: Alto Biobío samples; E and F: Santa Bárbara samples; G, H, I, and J: Hualqui samples; K, L, M, and N: Hualpén samples.

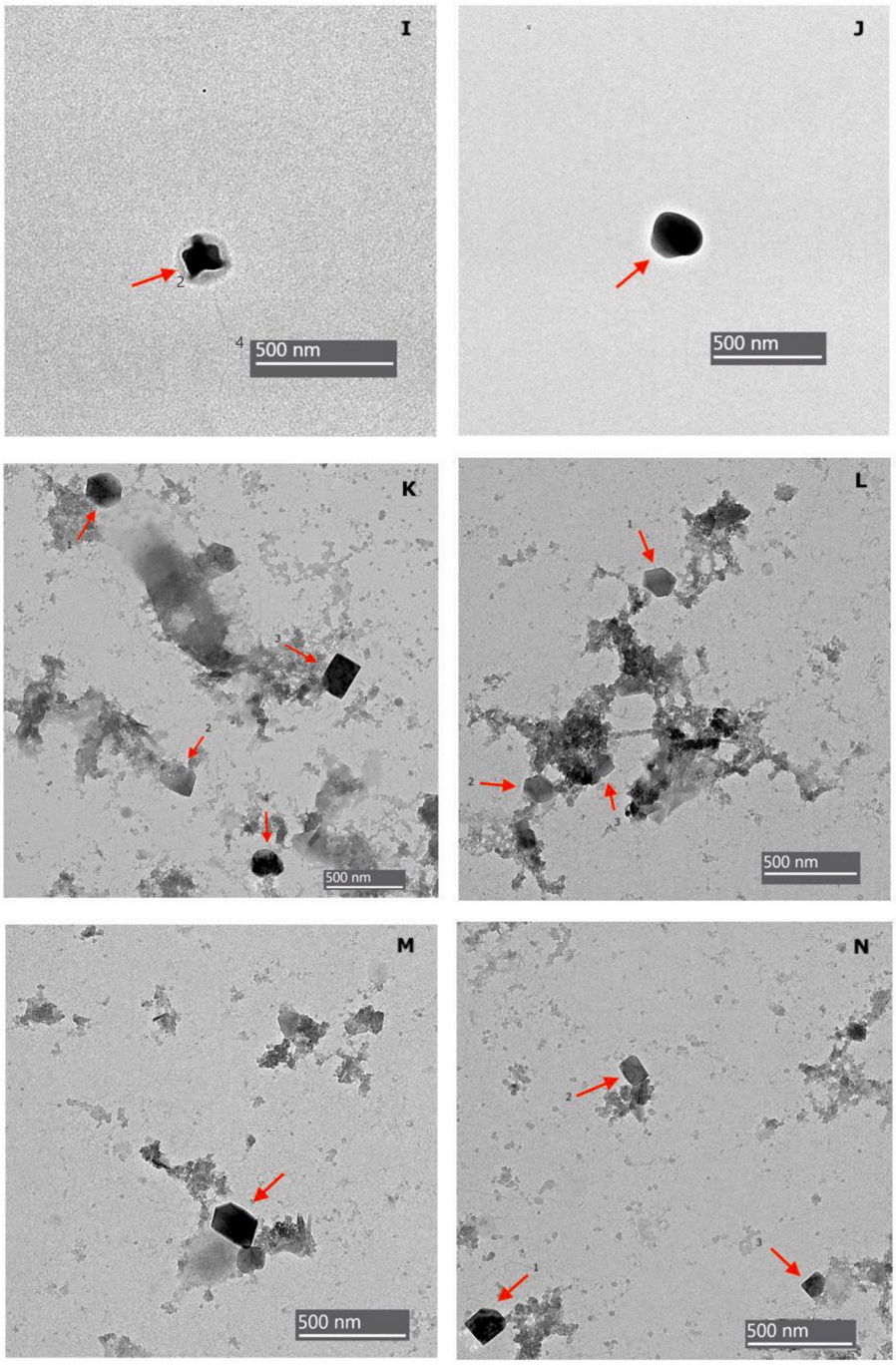

Fig. 6. (*continued*).

and 20.35 % of the dry weight. The brightest crystals were analyzed first and then the bottom of the sample, always finding the element present. Element mapping revealed a uniform presence of Ti in all samples indicating crystalline nature.

For the Hualpén sample, in Fig. 7-A, a cloud with bright spots is observed that indicates the presence of metals, similar to those observed in TEM when zooming in on the samples to reach nanometric scales, the spectrum scanned over the particles indicates the high Ti content present in the sample, as well as the presence of Fe and Al but to a lesser extent in the scanned point, these results agree with the ICP-MS analyzes where these same elements were observed predominantly, however at Through SEM-DLS it is possible to observe the nanoparticles present in the sample in a more localized way, so it can be discriminated when Ti predominates and confirm that the nanoparticles observed in TEM are Ti nanoparticles of anthropogenic origin.

According to the different sizes of TiO_2 nanoparticles observed in the water samples, it is important to note that we are in the presence of a potential environmental risk, a situation that can be extrapolated to countries demographically and geomorphologically similar to those seen in this research. Authors have described that size is crucial to determine whether synthetic nanoparticles have ecotoxicological effects; establishing that the size of 100 nm is considered a threshold to establish different levels of toxicity (Banerjee & Roychoudhury, 2019), because lengths less than 100 nm correspond to highly dangerous nanoparticles, since they can enter cells without any difficulty (Middepogu et al., 2018). On the other hand, nanoparticles between 100 and 200 nm have surface interactions with cells and can affect or limit cellular functions, thus causing malfunctions in their biochemical

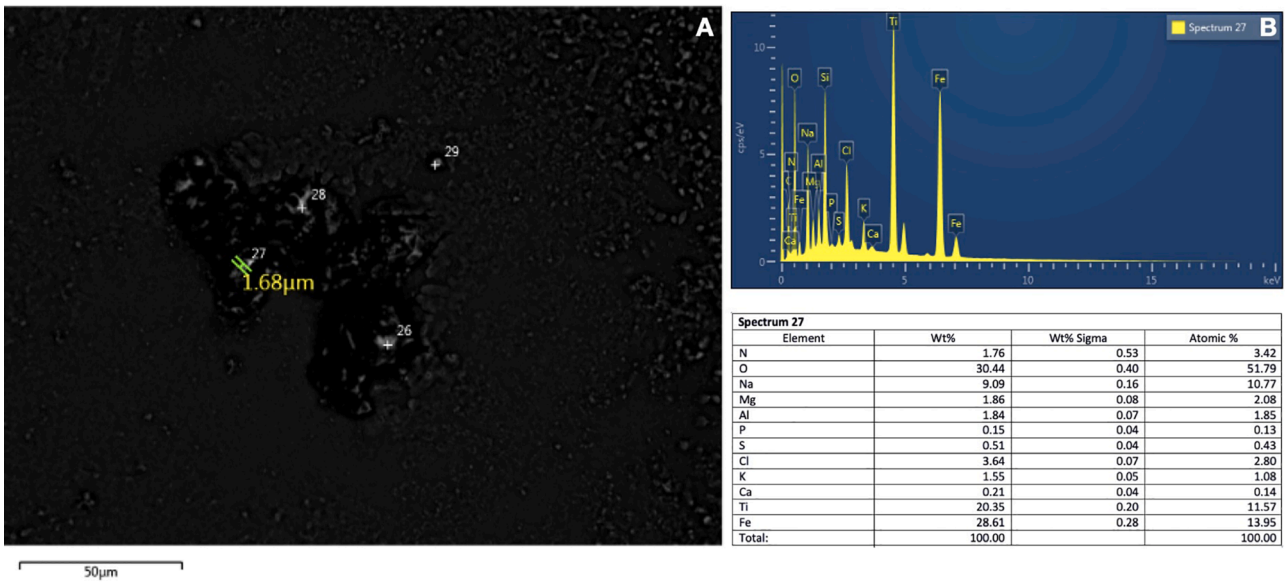

Spectrum 27			
Element	Wt%	Wt% Sigma	Atomic %
N	1.76	0.53	3.42
O	30.44	0.40	51.79
Na	9.09	0.16	10.77
Mg	1.86	0.08	2.08
Al	1.84	0.07	1.85
P	0.15	0.04	0.13
S	0.51	0.04	0.43
Cl	3.64	0.07	2.80
K	1.55	0.05	1.08
Ca	0.21	0.04	0.14
Ti	20.35	0.20	11.57
Fe	28.61	0.28	13.95
Total:	100.00		100.00

Fig. 7. Scanning electron microscope analysis with DLS element detector of Hualpén surface water. A: nanoparticle images obtained via SEM; B, spectrum that confirms the existence of elemental Ti.

processes (Perreault et al., 2012). Finally, nanoparticles with a size > 200 nm can aggregate or agglomerate, interacting with the same particle. According to what was mentioned above, in this study it was possible to identify all the size ranges that are potential environmental risk (see Table in annex D in complementary materials), taking a sense of urgency to establish baselines to establish the contributions of elements to surface water through of erosion or other natural processes to determine the concentration of possible xenobiotics that violate the stability of ecosystems through the ecotoxicological impacts of nanoparticles of anthropogenic origin.

4. Conclusion

Research on the presence and distribution of TiO_2 nanoparticles within the Biobío River has yielded definitive results. In the four strategically chosen sampling locations, our study has determined that the concentrations of TiO_2 nanoparticles varied significantly with seasonality, recording concentrations that ranged between 17.6 µg L^{-1} and 39.5 µg L^{-1}. These findings indicate a complex interaction between anthropogenic influences and natural river dynamics.

Using advanced TEM and VP-SEM analyses, we have observed a variety of nanoparticle shapes and sizes, demonstrating the diverse nature of TiO_2 nanoparticles in this river system. Our results have shown that nanoparticles found in river surface waters span sizes from 10 to 206 nm, and a significant proportion exist in the form of rutile and anatase.

Through precise ICP-MS and ICP measurements, we have quantified not only Ti but also associated trace elements such as Fe, Mn, and Al, further elucidating the physicochemical profile of the water samples. This comprehensive analytical approach has revealed a marked trend in the distribution and concentration of TiO_2 nanoparticles, suggesting possible sources and transport mechanisms.

The evidence suggests that TiO_2 nanoparticles are present along the river, regardless of proximity to urban activities, however an increase in concentrations is observed downstream of urban settlements, particularly defined structures corresponding to synthetic nanoparticles during the seasons. winter and spring. These findings highlight the river's role as a sink for TiO_2 nanoparticles, with possible implications for the ecology and human health of the basin.

This study provides a significant contribution to our understanding of nanodebris in aquatic environments, demonstrating the widespread distribution of TiO_2 nanoparticles in the Biobío River and establishing a clear seasonal pattern in their appearance. This research lays the foundation for future studies aimed at unraveling the complex fate and transport mechanisms of nanoparticles in aquatic ecosystems.

CRediT authorship contribution statement

Gester G. Gutiérrez: Writing – original draft, Writing – review & editing, Validation, Visualization, Resources, Software, Methodology, Project administration, Funding acquisition, Investigation, Conceptualization, Data curation, Formal analysis. **Alessandra Perfetti-Bolaño:** Data curation, Writing – review & editing. **Manuel Meléndrez:** Writing – review & editing, Methodology. **Karla Pozo:** Funding acquisition. **Ilaria Corsi:** Conceptualization, Methodology, Writing – review & editing. **Ricardo O. Barra:** Writing – review & editing, Conceptualization, Supervision. **Roberto Urrutia:** Writing – review & editing, Conceptualization, Investigation.

Declaration of competing interest

The authors declare the following financial interests/personal relationships which may be considered as potential competing interests:

Gester reports financial support was provided by National Agency for Research and Development. If there are other authors, they declare that they have no known competing financial interests or personal relationships that could have appeared to influence the work reported in this paper.

Acknowledgments

The research described in this document was funded by the National Agency for Research and Development of the Chilean government (ANID/FONDAP 15130015) through 2020 National Doctoral Scholarship N° 21200069, which supports the doctoral studies of author G. Gutiérrez. The authors also thank the EULA-Chile Environmental Science Center for contributing to the funding of this study. Special thanks to Dr. Allan Philippe of the University of Koblenz-Landau for sharing his extensive experience and contributions to the science of issues related to detection of nanoparticles in the environment. Dr. Pozo is grateful for Fondecyt project 1211931.

Supplementary materials

Supplementary material associated with this article can be found, in the online version, at doi:10.1016/j.envadv.2024.100536.

References

Akakuru, O.U., Iqbal, Z.M., Wu, A., 2020. TiO2 Nanoparticles. En *TiO2 Nanoparticles*. John Wiley & Sons, Ltd, pp. 1–66. https://doi.org/10.1002/9783527825431.ch1.

Albornoz Tapia, A.S., 2019. Estructura Del Basamento y su Posible Relación con la Actividad Holocena Del Volcán Antuco, Región del BioBío.

Ale, A., Liberatori, G., Vannuccini, M.L., Bergami, E., Ancora, S., Mariotti, G., Bianchi, N., Galdopórpora, J.M., Desimone, M.F., Cazenave, J., Corsi, I., 2019. Exposure to a nanosilver-enabled consumer product results in similar accumulation and toxicity of silver nanoparticles in the marine mussel Mytilus galloprovincialis. Aquat. Toxicol. 211, 46–56. https://doi.org/10.1016/j.aquatox.2019.03.018.

Azimzada, A., Farner, J.M., Hadioui, M., Liu-Kang, C., Jreije, I., Tufenkji, N., Wilkinson, K.J., 2020. Release of TiO 2 nanoparticles from painted surfaces in cold climates: Characterization using a high sensitivity single-particle ICP-MS. Environ. Sci.: Nano 7 (1), 139–148.

Baird, R., Bridgewater, L., 2017. Standard Methods for the Examination of Water and Wastewater, 23rd edition. American Public Health Association.

Banerjee, A., Roychoudhury, A., 2019. Nanoparticle-induced ecotoxicological risks in aquatic environments: concepts and controversies. Nanomater. Plant. Algae Microorgan. 129–141.

Bäuerlein, P.S., Emke, E., Tromp, P., Hofman, J.A., Carboni, A., Schooneman, F., de Voogt, P., van Wezel, A.P., 2017. Is there evidence for man-made nanoparticles in the Dutch environment? Sci. Tot. Environ. 576, 273–283.

Bhagat, J., Zang, L., Nishimura, N., Shimada, Y., 2020. Zebrafish: An emerging model to study microplastic and nanoplastic toxicity. Sci. Tot. Environ. 728, 138707 https://doi.org/10.1016/j.scitotenv.2020.138707.

Boenisch, K., 2020. Environmental Transformations in Hydrophobicity of TiO2 P-25 Nanoparticles in Alsea River Waters.

Campos, D.A., Schaumann, G.E., Philippe, A., 2022. Natural TiO_2-nanoparticles in soils: a review on current and potential extraction methods. Crit. Rev. Anal. Chem. 52 (4), 735–755. https://doi.org/10.1080/10408347.2020.1823812.

Caro, R., 2004. Diagnóstico y Clasificación de los Cursos y Cuerpos de agua según Objetivos de calidad: Informe final, año 2004.

Cascio, C., Geiss, O., Franchini, F., Ojea-Jimenez, I., Rossi, F., Gilliland, D., Calzolai, L., 2015. Detection, quantification and derivation of number size distribution of silver nanoparticles in antimicrobial consumer products. J. Anal. At. Spectrom. 30 (6), 1255–1265.

Corporación Nacional Forestal, C., 2020. Sistema de Información Territorial. https://sit.conaf.cl/.

Deng, X.-Y., Cheng, J., Hu, X.-L., Wang, L., Li, D., Gao, K., 2017. Biological effects of TiO2 and CeO2 nanoparticles on the growth, photosynthetic activity, and cellular components of a marine diatom Phaeodactylum tricornutum. Sci. Tot. Environ. 575, 87–96.

DGA, O., 2022. Información Pluviométrica, Fluviométrica, Estado de Embalses y Aguas Subterráneas. https://dga.mop.gob.cl/productosyservicios/informacionhidrologica/Paginas/default.aspx.

Díaz, M.E., Figueroa, R., Alonso, M.L.S., Vidal-Abarca, M.R., 2018. Exploring the complex relations between water resources and social indicators: the Biobío Basin (Chile). Ecosyst. Serv. 31, 84–92. https://doi.org/10.1016/j.ecoser.2018.03.010.

dos Santos, C.A., Ingle, A.P., Rai, M., 2020. The emerging role of metallic nanoparticles in food. Appl. Microbiol. Biotechnol. 104 (6), 2373–2383. https://doi.org/10.1007/s00253-020-10372-x.

Fan, G., You, Y., Wang, B., Wu, S., Zhang, Z., Zheng, X., Bao, M., Zhan, J., 2019. Inactivation of harmful cyanobacteria by Ag/AgCl@ ZIF-8 coating under visible light: Efficiency and its mechanisms. Appl. Cataly. B: Environ. 256, 117866.

Farshbaf, M., Valizadeh, H., Panahi, Y., Fatahi, Y., Chen, M., Zarebkohan, A., Gao, H., 2022. The impact of protein corona on the biological behavior of targeting nanomedicines. Int. J. Pharm. 614, 121458 https://doi.org/10.1016/j.ijpharm.2022.121458.

Greber, N.D., Pettke, T., Vilela, N., Lanari, P., Dauphas, N., 2021. Titanium isotopic compositions of bulk rocks and mineral separates from the Kos magmatic suite: Insights into fractional crystallization and magma mixing processes. Chem. Geol. 578, 120303 https://doi.org/10.1016/j.chemgeo.2021.120303.

Hajizadeh-Oghaz, M., 2019. Synthesis and characterization of Nb-La co-doped TiO2 nanoparticles by sol-gel process for dye-sensitized solar cells. Ceram. Int. 45 (6), 6994–7000. https://doi.org/10.1016/j.ceramint.2018.12.200.

Henriquez, F., 1978. Posibilidades de Subproductos en la Minería del Hierro en Chile.

Iadonisi, G., Cantele, G., Chiofalo, M.L., 2014. Introduction to Solid State Physics and Crystalline Nanostructures. Springer.

Keller, A.A., Wang, H.T., Zhou, D.X., Lenihan, H.S., Cherr, G., Cardinale, B.J., Miller, R., Ji, Z.X., 2010. Stability and aggregation of metal oxide nanoparticles in natural aqueous matrices. Environ. Sci. Technol. 44 (6), 1962.

Khan, J.A., Sayed, M., Shah, N.S., Khan, S., Khan, A.A., Sultan, M., Tighezza, A.M., Iqbal, J., Boczkaj, G., 2023. Synthesis of N-doped TiO_2 nanoparticles with enhanced photocatalytic activity for 2,4-dichlorophenol degradation and H_2 production. J. Environ. Chem. Eng. 11 (6), 111308 https://doi.org/10.1016/j.jece.2023.111308.

Khan, J.A., Sayed, M., Shah, N.S., Khan, S., Zhang, Y., Boczkaj, G., Khan, H.M., Dionysiou, D.D., 2020. Synthesis of eosin modified TiO_2 film with co-exposed {001} and {101} facets for photocatalytic degradation of para-aminobenzoic acid and solar H_2 production. Appl. Cataly. B: Environ. 265, 118557 https://doi.org/10.1016/j.apcatb.2019.118557.

Kim, E., Kim, S.-H., Kim, H.-C., Lee, S.G., Lee, S.J., Jeong, S.W., 2011. Growth inhibition of aquatic plant caused by silver and titanium oxide nanoparticles. Toxicol. Environ. Health Sci. 3, 1–6.

Labille, J., Harns, C., Bottero, J.-Y., Brant, J., 2015. Heteroaggregation of titanium dioxide nanoparticles with natural clay colloids. Environ. Sci. Technol. 49 (11), 6608–6616. https://doi.org/10.1021/acs.est.5b00357.

Latif, S., Tahir, K., Khan, A.U., Abdulaziz, F., Arooj, A., Alanazi, T.Y., Rakic, V., Khan, A., Jevtovic, V., 2022. Green synthesis of Mn-doped TiO_2 nanoparticles and investigating the influence of dopant concentration on the photocatalytic activity. Inorg. Chem. Commun. 146, 110091.

Liao, D.L., Liao, B.Q., 2007. Shape, size and photocatalytic activity control of TiO2 nanoparticles with surfactants. J. Photochem. Photobiol. A: Chem. 187 (2), 363–369. https://doi.org/10.1016/j.jphotochem.2006.11.003.

Middepogu, A., Hou, J., Gao, X., Lin, D., 2018. Effect and mechanism of TiO_2 nanoparticles on the photosynthesis of Chlorella pyrenoidosa. Ecotoxicol. Environ. Saf. 161, 497–506.

Mohamed, M.M., Othman, I., Mohamed, R., 2007. Synthesis and characterization of $MnOx/TiO_2$ nanoparticles for photocatalytic oxidation of indigo carmine dye. J. Photochem. Photobiol. A: Chem. 191 (2-3), 153–161.

Morais, R.P., Hochheim, S., Oliveira, C.C.de, Riegel-Vidotti, I.C., Marino, C.E.B., 2022. Skin interaction, permeation, and toxicity of silica nanoparticles: Challenges and recent therapeutic and cosmetic advances. Int. J. Pharm. 614, 121439 https://doi.org/10.1016/j.ijpharm.2021.121439.

Morelli, E., Gabellieri, E., Bonomini, A., Tognotti, D., Grassi, G., Corsi, I., 2018. TiO2 nanoparticles in seawater: Aggregation and interactions with the green alga Dunaliella tertiolecta. Ecotoxicol. Environ. Saf. 148, 184–193. https://doi.org/10.1016/j.ecoenv.2017.10.024.

Nabi, M.M., Wang, J., Baalousha, M., 2021. Episodic surges in titanium dioxide engineered particle concentrations in surface waters following rainfall events. Chemosphere 263, 128261. https://doi.org/10.1016/j.chemosphere.2020.128261.

Oukarroum, A., Barhoumi, L., Pirastru, L., Dewez, D., 2013. Silver nanoparticle toxicity effect on growth and cellular viability of the aquatic plant Lemna gibba. Environ. Toxicol. Chem. 32 (4), 902–907.

Perreault, F., Oukarroum, A., Melegari, S.P., Matias, W.G., Popovic, R., 2012. Polymer coating of copper oxide nanoparticles increases nanoparticles uptake and toxicity in the green alga Chlamydomonas reinhardtii. Chemosphere 87 (11), 1388–1394.

Philippe, A., Bazoobandi, A., Goeppert, N., 2022. Quantification of anthropogenic TiO2 nanoparticles in soils and sediments combining size fractionation and trace element ration. J. Anal. At. Spectrom. 37 (2), 338–350.

Philippe, A., Campos, D.A., Guigner, J.-M., Buchmann, C., Diehl, D., Schaumann, G.E., 2018. Characterization of the Natural Colloidal TiO2 Background in Soil. Separations. 5 (4) https://doi.org/10.3390/separations5040050.

Rai, M., Ingle, A.P., Gupta, I., Pandit, R., Paralikar, P., Gade, A., Chaud, M.V., dos Santos, C.A., 2019. Smart nanopackaging for the enhancement of food shelf life. Environ. Chem. Lett. 17 (1), 277–290. https://doi.org/10.1007/s10311-018-0794-8.

Rajput, V.D., Singh, A., Minkina, T., Rawat, S., Mandzhieva, S., Sushkova, S., Shuvaeva, V., Nazarenko, O., Rajput, P., Komariah, 2021. Nano-enabled products: Challenges and opportunities for sustainable agriculture. Plants 10 (12), 2727.

Rozas, O., Vidal, C., Baeza, C., Jardim, W.F., Rossner, A., Mansilla, H.D., 2016. Organic micropollutants (OMPs) in natural waters: Oxidation by UV/H2O2 treatment and toxicity assessment. Water. Res. 98, 109–118. https://doi.org/10.1016/j.watres.2016.03.069.

Santás-Miguel, V., Arias-Estévez, M., Rodríguez-Seijo, A., Arenas-Lago, D., 2023. Use of metal nanoparticles in agriculture. A review on the effects on plant germination. Environ. Pollut., 122222

Sengupta, A., Sarkar, C.K., 2015. Introduction to Nano: Basics to Nanoscience and Nanotechnology. Springer.

Stegemeier, J.P., Colman, B.P., Schwab, F., Wiesner, M.R., Lowry, G.V., 2017. Uptake and distribution of silver in the aquatic plant Landoltia punctata (duckweed) exposed to silver and silver sulfide nanoparticles. Environ. Sci. Technol. 51 (9), 4936–4943.

Sukhdev, A., Challa, M., Narayani, L., Manjunatha, A.S., Deepthi, P.R., Angadi, J.V., Kumar, P.M., Pasha, M., 2020. Synthesis, phase transformation, and morphology of hausmannite Mn3O4 nanoparticles: Photocatalytic and antibacterial investigations. Heliyon. 6 (1), e03245. https://doi.org/10.1016/j.heliyon.2020.e03245.

Vargas Urbano, M.A., Ochoa Muñoz, Y.H., Ortegón Fernández, Y., Mosquera, P., Rodríguez Páez, J.E., Camargo Amado, R.J., 2011. Nanopartículas de TiO2, fase anatasa, sintetizadas por métodos químicos. Ingeniería y Desarrollo 29 (2), 186–201.

Vera, I., Sáez, K., Vidal, G., 2013. Performance of 14 full-scale sewage treatment plants: Comparison between four aerobic technologies regarding effluent quality, sludge production and energy consumption. Environ. Technol. 34 (15), 2267–2275. https://doi.org/10.1080/09593330.2013.765921.

Vidmar, J., Zuliani, T., Milačič, R., Ščančar, J., 2022. Following the occurrence and origin of titanium dioxide nanoparticles in the Sava river by single particle ICP-MS. Water (Basel) 14 (6), 959.

Westerhoff, P., Song, G., Hristovski, K., Kiser, M.A., 2011. Occurrence and removal of titanium at full scale wastewater treatment plants: Implications for TiO 2 nanomaterials. J. Environ. Monitor. 13 (5), 1195–1203.

Yadav, G., Ahmaruzzaman, Md, 2022. Consumer nanoproducts: a brief introduction. In: Mallakpour, En S., Hussain, C.M. (Eds.), Handbook of Consumer Nanoproducts.

Springer Nature, Singapore, pp. 3–16. https://doi.org/10.1007/978-981-16-8698-6_85.

Yevenes, M.A., Figueroa, R., Parra, O., 2018. Seasonal drought effects on the water quality of the Biobío River, Central Chile. Environ. Sci. Pollut. Res. 25 (14), 13844–13856. https://doi.org/10.1007/s11356-018-1415-6.

Zhang, Q., Hu, Y., Masterson, C.M., Jang, W., Xiao, Z., Bohloul, A., Garcia-Rojas, D., Puppala, H.L., Bennett, G., Colvin, V.L., 2022. When function is biological: Discerning how silver nanoparticle structure dictates antimicrobial activity. iScience 25 (7), 104475. https://doi.org/10.1016/j.isci.2022.104475.